Chemistry–A European Journal
Research Article
doi.org/10.1002/chem.202104318
Chemistry Europe
European Chemical Societies Publishing
www.chemeurj.org

Hydrogen-Bridged Oligosilanylsilyl Mono- and Oligosilanylsilyl Dications

Jelte P. Nimoth[a] and Thomas Müller*[a]

Abstract: Hydrogen-bridged oligosilanylsilyl borates **8**[B-$(C_6F_5)_4$], **9**[$B(C_6F_5)_4$] and diborates **10**[$B(C_6F_5)_4]_2$ have been prepared by hydride transfer between α-ω-dihydrido- (**11**) and branched tetrahydrido-oligosilanes (**13**) and trityl cation. The obtained cyclic intramolecularly stabilized silylium ions **8**, **9** and *bis*silylium ion **10** were characterized by low temperature NMR spectroscopy supported by the results of density functional calculations. The branched Si–H–Si monocation **9** undergoes at low temperatures a fast degenerate rearrangement, which exchanges the Si–H groups with a barrier of 31 kJ mol^{-1} via an *antarafacial* transition state. Reaction of the branched monocation **9** with a second equivalent of trityl cation or of the branched oligosilane **13** with two equivalents of trityl cation, gives at −80 °C the corresponding *bis*silylium ion **10**, an example for a new class of highly reactive poly-Lewis acids.

Introduction

Silyl cations in general and silylium ions in particular can be classified as *Lewis super acids* due to their exceptionally high Lewis acidity.[1] Examples for tricoordinated silylium ions of the type $[R_3Si]^+$ are rare,[2–5] but their immense reactivity and Lewis acidity is attenuated by coordination of donor molecules, for example anions or solvent molecules, or by the intramolecular coordination of Lewis basic groups.[6] In this way, their Lewis acidity and reactivity can be controlled and, in some cases, even fine-tuned to suit the desired application.[7] An interesting mode, which conserves much of the original reactivity, is the stabilization of silylium ions by silanes through the formation of inter- or intramolecular 3c2e Si–H–Si bridges. Historically, the cyclic silyl cation **1** (Figure 1), obtained by a hydride transfer reaction[8,9] from an α,ω-*bis*hydridosilyl carbosilane, was the first well documented example for such an interaction between a silane and a silylium ion.[10] During the last twenty years, additional examples of silylium ions that are stabilized by intramolecular 3c2e Si–H–Si bridges were characterized by NMR spectroscopy or X-ray diffraction (XRD) analysis.[11–15] It became also evident that the hydride transfer reaction of trialkylhydridosilanes in an excess of silane as solvent does not lead to the respective silylium ions, as initially proposed,[16,17] but results in the formation of the intermolecularly Si–H–Si bridged species.[18,19] This result underlined the general importance of this stabilization mode in silylium ion chemistry and the parallels to the activation of silanes by neutral boron or aluminum Lewis acids are obvious.[20–24] In further studies, the utility of 3c2e Si–H–Si bridges was demonstrated by using Si–H functionalities to trap intramolecularly silylium intermediates in sila-Wagner–Meerwein rearrangements of oligosilanes.[12,13] Although the silane/silylium ion interaction has been well studied by several research groups, the interaction between silylium ions and multiple Si–H groups (polyagostic interaction) has been investigated only in the case of spatially restricted polysilylarene derived cations **2** and **3** (Figure 1).[25,26] Cyclic Si–H–Si bridged cations seemed to be perfect precursors for the synthesis of *bis*silylium ions, a novel class of bidentate Lewis acids.[27–29] First attempts to use the Si–H–Si stabilized cation **4**

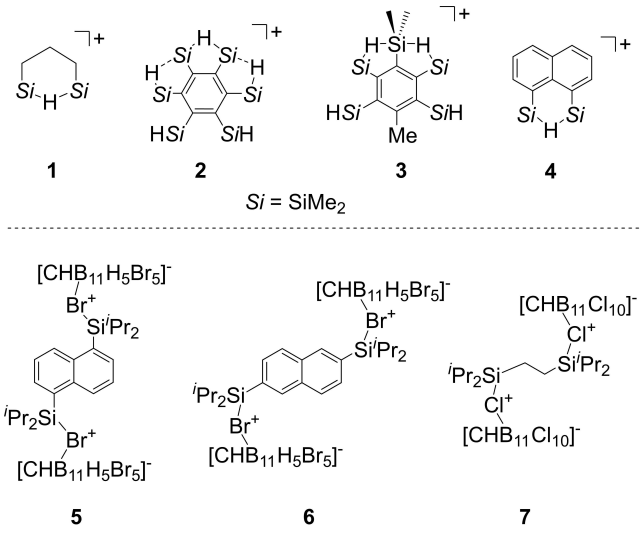

Figure 1. Selected examples of Si–H–Si bridged silyl monocations **1**–**4** and examples for anion stabilized bissilylium ions **5**–**7**.

[a] *Dr. J. P. Nimoth, Prof. Dr. T. Müller*
Institute of Chemistry
Carl von Ossietzky University Oldenburg
Carl von Ossietzky-Str. 9–11, 26129
Oldenburg (Germany, European Union)
E-mail: thomas.mueller@uol.de

Supporting information for this article is available on the WWW under https://doi.org/10.1002/chem.202104318

(Figure 1) as precursor for a potent bidentate *bis*silyl Lewis acid were unsuccessful in so far as the high reactivity of the generated dication decomposed the weakly coordinating [B-$(C_6F_5)_4]^-$ anion.[14]

Recently, the Oestreich group succeeded in taming *bis*silylium ions **5**–**7** (Figure 1) by using halogenated carborate anions as external stabilizing donors, starting from either spatially well separated *bis*hydridosilanes (for dications **5** and **6**) or small cyclic Si–H–Si bridged cations (in the case of **7**).[30] In the present work, we describe the results of our systematic study on a series of intramolecularly stabilized silyl cations, all featuring one or two six-membered cationic $[Si_5H]^+$ rings. This includes the persila-variant **8** of cation **1**, the interaction of the cationic Si–H–Si bridge with additional Si–H functionalities in the branched oligosilanylsilyl cation **9** and its transformation to dication **10** as an example for a *bis*silyl Lewis acid that is stabilized only by silane/silylium interaction (Figure 2).[30–32]

Results and Discussion

The synthesis of starting material $HMe_2Si(SiMe_2)_3SiMe_2H$ (**11**) was achieved by a series of salt metathesis steps involving $PhMe_2SiLi$[33] followed by a protiodephenylation reaction of oligosilane **12** via silyl triflates and final introduction of the Si–H functionalities by lithium alanate (Scheme 1).[34] Similarly, the branched oligosilane $Si(SiMe_2SiMe_2H)_4$ (**13**) was obtained via protiodephenylation of the tetraphenyl substituted oligosilane **14** followed by triflate to hydride substitution. The latter was synthesized in excellent yields (up to 86%) and high purity by multiple silyl group exchange, a protocol reported previously by the Marschner group (Scheme 1).[35]

The newly synthesized silanes **11** and **13** were characterized by NMR spectroscopy, and mass spectrometry. The molecular structure of oligosilane **14** was further examined by XRD analysis (see Supporting Information for details). UV/vis analysis of **14** revealed an intensive long wavelength absorption at 252 nm reminiscent of the 255 nm reported for **12** (Scheme 1).[36] This result rules out a significant influence of the branching at the central Si atom on the σ-conjugation.[37,38] The isolated oligosilanes **11** and **13** were used for cation synthesis by reaction with $[Ph_3C][B(C_6F_5)_4]$ to form the respective oligosilanylsilyl borates (Corey reaction, Scheme 2). All reactions had to be performed at low temperatures as the reactions of both oligosilanes with trityl borate using standard Corey

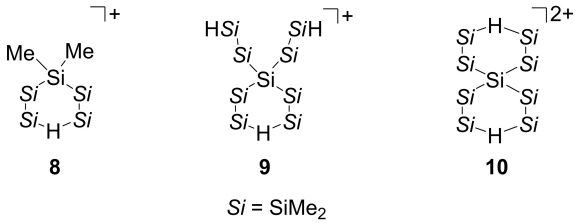

Figure 2. Oligosilanylsilyl cations **8**, **9** and dication **10** discussed in this work.

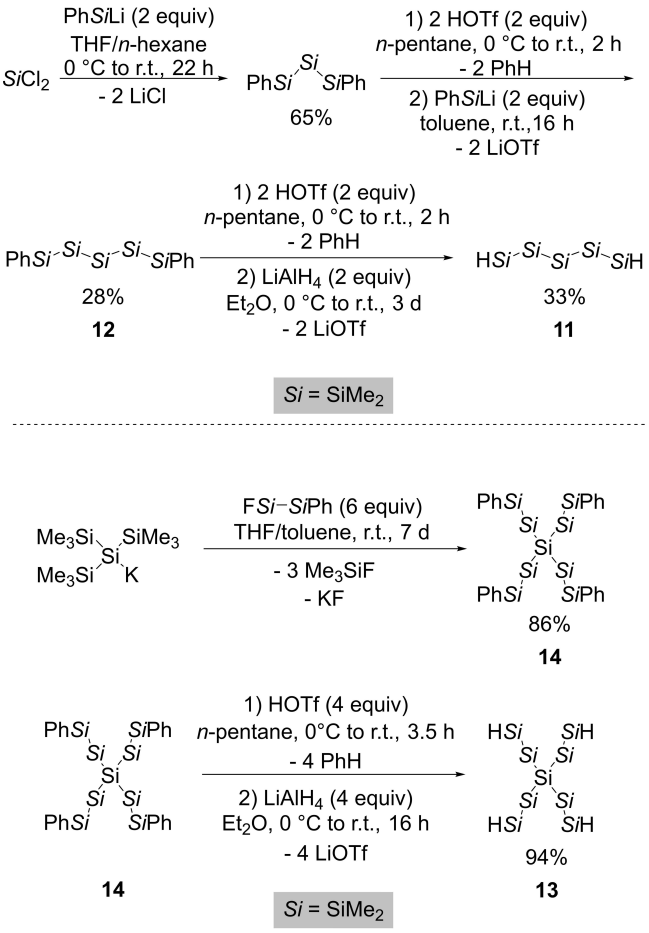

Scheme 1. Synthesis of hydrogen-substituted oligosilanes **11** and **13**.

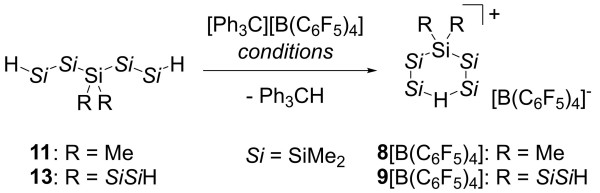

R	Silane	Cation	*conditions*
Me	**11**	**8**	C_6D_5Cl, –40 °C
Me	**11**	**8**	CD_2Cl_2, –90 °C
*SiSi*H	**13**	**9**	CD_2Cl_2, –90 °C

Scheme 2. Synthesis of *bis*silylhydronium borates **8**$[B(C_6F_5)_4]$ and **9**$[B(C_6F_5)_4]$ from oligosilanes **11** and **13**.

conditions (room temperature, aromatic hydrocarbons or halohydrocarbons) resulted in intractable product mixtures.

After reaction of the linear silane **11** with $[Ph_3C][B(C_6F_5)_4]$ in chlorobenzene-d_5 at T = −40 °C (Scheme 2), we observed the selective formation of the intramolecularly silane-stabilized silylium ion **8**. Only three NMR signals are detected in the ^{29}Si NMR spectrum at this temperature (Table 1, Figures S31–S34). While the ^{29}Si nuclei of the $SiMe_2$ groups in position 1 and 2 of

Table 1. Experimental NMR data of Si–H–Si bridged silyl cations **8**–**10**. Computed ^{29}Si NMR chemical shifts[a] and $^{1}J_{Si,H}$ coupling constants[b] are given in parenthesis.

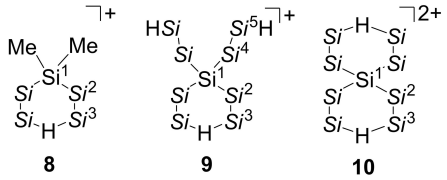

8 **9** **10**

Si = $SiMe_2$

Cation	Group	δ^{1}H[c]	δ^{13}C[c]	δ^{29}Si
8[d]	Si^1	0.10	−7.1	−38.1 (−35)
	Si^2	0.13	−7.7	−43.3 (−42)
	Si^3	0.39	−2.5	87.1 (95)
		0.44[g]		$^{1}J_{Si,H}$ = 37 Hz (48 Hz)
8[e]	Si^1	0.30	–[h]	−37.6
	Si^2	0.35	–[h]	−43.4
	Si^3	0.80	–[h]	87.3
		0.73[g]		
9[e]	Si^1	–	–	−124.8 (−120)
	Si^2	–[j]	–[j]	−37.1/−35.0[k] (−35)
	Si^3	–[j]	–[j]	89.1 (97) $^{1}J_{Si,H}$ = 31 Hz[l] (49 Hz)
	Si^4	–[j]	–[j]	−37.1/−35.0[k] (−34)
	Si^5	–[j]	–[j]	−34.3 (−33)[n] $^{1}J_{Si,H}$ = 170 Hz[m] (176 Hz)[n]
10[f]	Si^1	–	–	−121.4 (−116)
	Si^2	0.55	−3.1	−34.4 (−34)
	Si^3	0.89	−2.2	88.1 (96)
		0.81[g]		$^{1}J_{Si,H}$ = 41 Hz (47 Hz)

[a] Calculated at GIAO/M06-L/6-311G(2d,p)//M06-2X/6-311+G(d,p). [b] Calculated at B3LYP/IGLOIII//M06-2X/6-311+G(d,p). [c] NMR shifts of Me groups at Si^X. [d] C_6D_5Cl, −40 °C. [e] CD_2Cl_2, −90 °C. [f] CD_2Cl_2, −80 °C. [g] Bridging H atom detected by $^{1}H,^{29}Si$ HMQC spectroscopy. [h] Not measured. [j] NMR signals too broad to allow an assignment. [k] Distinction between Si^2/Si^4 by NMR not possible. [l] Detection at −93 °C. [m] Due to overlapping signals the reported coupling constant has an uncertainty of ±5 Hz. [n] Mean value calculated for the two magnetically not isochronous $SiMe_2H$ groups.

the six-membered $[Si_5H]^+$ cycle resonate at very similar frequencies as the respective groups in the neutral precursor **11**,[39] the 3c2e Si–H–Si bridge is clearly assigned by its downfield-shifted signal at $\delta^{29}Si^3$ = 87.1. For this signal, a markedly reduced Si–H coupling constant of $^{1}J_{Si,H}$ = 37 Hz is detected in the hydrogen-coupled ^{29}Si INEPT NMR spectrum (Figure 3, insert). The ^{1}H and ^{13}C NMR data are also in agreement with the proposed cyclic, Si–H–Si bridged structure (Table 1). The ^{1}H NMR chemical shift of the bridging hydrogen atom of **8** (δ^{1}H = 0.44 in C_6D_5Cl) was determined from the $^{1}H,^{29}Si$ HMQC spectrum (Figure 3). Finally, the results of the ^{29}Si NMR chemical shift calculations confirm our assignment based on the NMR experiments (Table 1).

We repeated the reaction in dichloromethane-d_2 to investigate possible solvent interactions. For the ^{1}H NMR shifts, we observed a shift downfield by about $\Delta(\delta^{1}H)$ = 0.20–0.40 while

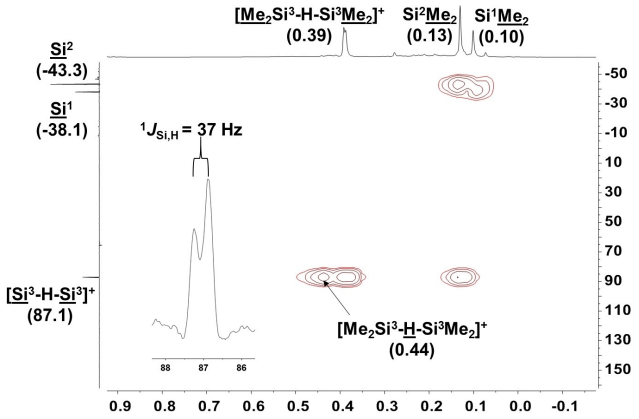

Figure 3. $^{1}H,^{29}Si$ HMQC spectrum of **8**$[B(C_6F_5)_4]$ (C_6D_5Cl, −40 °C, 499.87 MHz, parameters for J = 45 Hz). Insert: Splitting of the signal at $\delta^{29}Si$ = 87.1 in the ^{29}Si INEPT NMR spectrum (C_6D_5Cl, −40 °C, 99.31 MHz).

the ^{29}Si NMR chemical shifts in both solvents are practically identical (Table 1). Based on these results, we rule out structure-determining interactions between silyl cation **8** and chlorinated hydrocarbons, in agreement with previous studies on intramolecularly Si–H–Si bridged cations.[10,12,14]

At temperatures slightly higher than −80 °C, we observed in dichloromethane-d_2 the selective formation of the corresponding *bis*silylchloronium borate **15**$[B(C_6F_5)_4]$ from the Si–H–Si bridged cation **8**. This observation demonstrates the high reactivity of **8** (Scheme 3, see Supporting Information for details).

Subsequently, the hydride transfer reaction between the branched oligosilane **13** and one equivalent of $[Ph_3C][B(C_6F_5)_4]$ was performed in dichloromethane-d_2 at T = −90 °C (Scheme 2). The obtained NMR spectroscopic data are in accordance with a highly dynamic behavior of cation **9** on the NMR time scale even at T = −90 °C. The ^{1}H NMR and $^{13}C\{^{1}H\}$ NMR spectra are dominated by broad featureless signals that prevent a detailed analysis (Figures S52–S54). Therefore, the structural assignment of the formed silyl cation primarily relies on the ^{29}Si NMR spectroscopic data (Table 1). In the $^{29}Si\{^{1}H\}$ NMR spectrum of cation **9** (Figure 4, top spectrum), five signals are detected. The most upfield-shifted signal at $\delta^{29}Si$ = −124.8 is assigned to the central silicon atom Si^1 by comparison with the starting material **13** ($\delta^{29}Si$ = −119.2). The broad resonance of the Si^3 atoms appear at $\delta^{29}Si$ = 89.1 (line width at half height, $\omega_{1/2}$ = 62 Hz) and it shows no detectable $^{1}J_{Si,H}$ splitting in the ^{29}Si NMR spectrum at the same temperature (Figure 4, bottom spectrum). Upon cooling of the sample down to T = −93 °C, the downfield signal

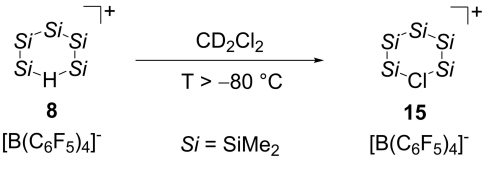

Scheme 3. Formation of **15**$[B(C_6F_5)_4]$ in dichloromethane.

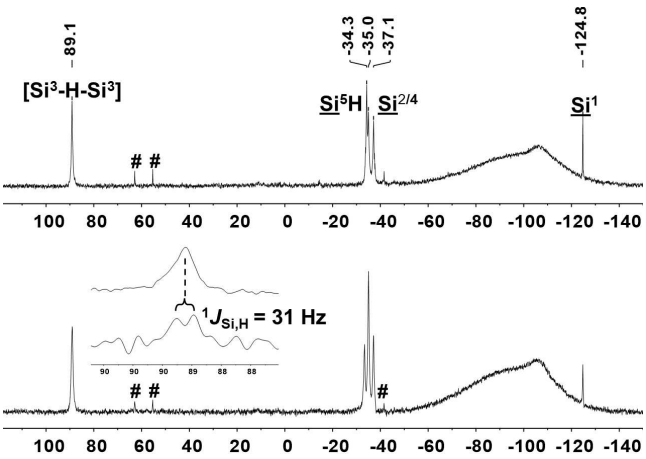

Figure 4. $^{29}Si\{^1H\}$ (top) and ^{29}Si NMR (bottom) spectra of **9**$[B(C_6F_5)_4]$ (CD_2Cl_2, −90 °C, 99.31 MHz, # = unidentified side-products). Insert: Part of the ^{29}Si NMR spectra showing the doublet splitting of the downfield ^{29}Si resonance at T = −93 °C.

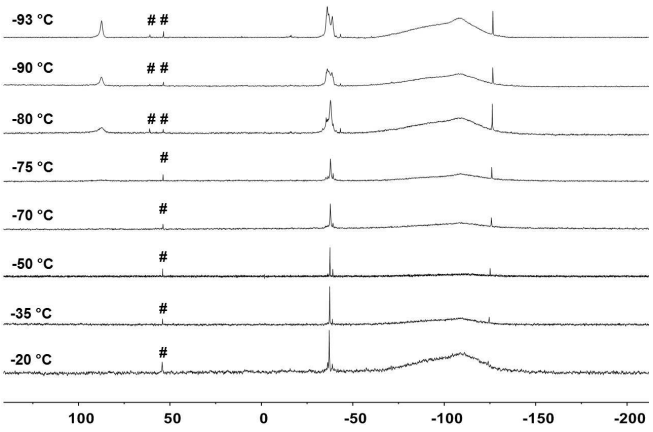

Figure 5. VT $^{29}Si\{^1H\}$ NMR spectra of **9**$[B(C_6F_5)_4]$ (CD_2Cl_2, VT, 99.31 MHz, # = unidentified side-products).

sharpens ($\omega_{1/2}$ = 43 Hz) and a doublet splitting of $^1J_{Si,H}$ = 31 Hz becomes visible (Figure 4, insert in the bottom spectrum). Even at this temperature, the broad signals in the ^1H and $^{13}C\{^1H\}$ NMR spectra of **9** make an exact assignment of the signals impossible. Hence, the position of the signal of the bridging hydrogen atom cannot be detected by either 1D or 2D NMR spectroscopy. The silicon atom Si^5 resonates at $\delta^{29}Si$ = −34.3 and splits up into a doublet in the hydrogen-coupled ^{29}Si NMR spectrum ($^1J_{Si,H}$ = 170 Hz, see Supporting Information for details). The observed $^1J_{Si,H}$ coupling is almost identical to the one detected for the neutral starting material **12** ($^1J_{Si,H}$ = 178 Hz). The remaining two signals are broad singlets in the ^{29}Si NMR spectrum at T = −90 °C and are assigned to the silicon atoms Si^2 and Si^4. A distinction based on the experimental data is not possible. The results of ^{29}Si NMR chemical shift calculations support our structural assignment (Table 1).

We note here that the decisive NMR spectroscopic parameters of branched cation **9** are very similar to those of the monocyclic cation **8** (Table 1). There is no indication of an additional interaction of the non-bridging Si–H groups with the cationic Si–H–Si bridge in the ground state. For example, no reduced Si–H coupling constant is detected for the additional hydridosilane groups.[25,26] Variable temperature (VT) $^{29}Si\{^1H\}$ NMR experiments reveal a strong dependency of the number of signals on the temperature (Figure 5).

With increasing temperature, the signals at $\delta^{29}Si$ = 89.0 (Si^3) and −34.2 (Si^5) broaden and finally disappear at T = −70 °C. No averaged ^{29}Si NMR signal is detected for $Si^{3/5}$ up to T = −20 °C. At the same time, the signals at $\delta^{29}Si$ = −37.2 and −35.1 (Si^2 and Si^4) broaden and an averaged signal at $\delta^{29}Si$ = −36.6 appears (Figure 5). The underlying process is shown to be reversible upon renewed cooling (see Supporting Information for details). These observations suggest an intramolecular, reversible hydride transfer between the terminal dimethylsilyl groups and the dimethylsilyl groups that are involved in the Si–H–Si moieties of cation **9**. This process equilibrates the Si atoms in α position (Si^3 and Si^5) and atoms in β position (Si^2 and Si^4), respectively (Scheme 4).

The barrier of this process can be estimated from the VT ^{29}Si NMR data to be as low as $\Delta G^{\neq,exp}$ = 31 kJ mol^{-1} (see Supporting Information, ch. 5). At T = −20 °C, the ^1H NMR spectrum shows first signs of decomposition which becomes rapid around T = 0 °C and results in a mixture of unidentifiable products (see Figure S113). The ^1H NMR data at increased temperatures support the dynamic process. Thus, three signals are visible in the ^1H NMR spectrum T = −30 °C (see Figures S109–S111): A broad singlet at δ^1H = 2.89 and two singlets at δ^1H = 0.45/0.55 whose integral ratio of 3H (δ^1H = 2.89) : 24H (δ^1H = 0.55) : 24H (δ^1H = 0.45) agrees with an averaging of the ^1H NMR signals of all four disilyl units of **9** (Scheme 4).

The formation of cation **9** was further verified by a trapping reaction between silyl borate **9**$[B(C_6F_5)_4]$ and $^nBu_3SnD$ at T = −40 °C in toluene which resulted in the formation of the neutral, monodeuterated starting material **13**-D_1 (Scheme 5, Supporting Information material, ch. 4).

The reaction of **13** with two equivalents of $[Ph_3C][B(C_6F_5)_4]$ led even at T = −80 °C to a spontaneous decoloration of the reaction mixture which indicates the complete consumption of the trityl cation and the formation of the dication **10** (Scheme 6).

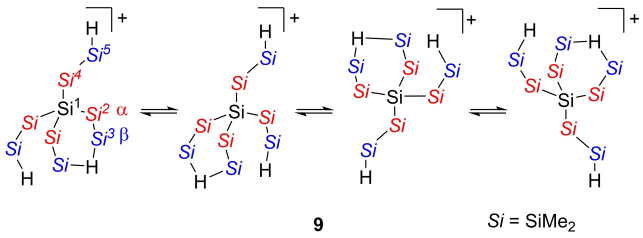

Scheme 4. Schematic representation of the degenerate intramolecular hydride transfer of cation **9** that equilibrates the silicon atoms Si^2 and Si^4, and the silicon atoms Si^3 and Si^5. The $[B(C_6F_5)_4]^-$ counter anion is omitted.

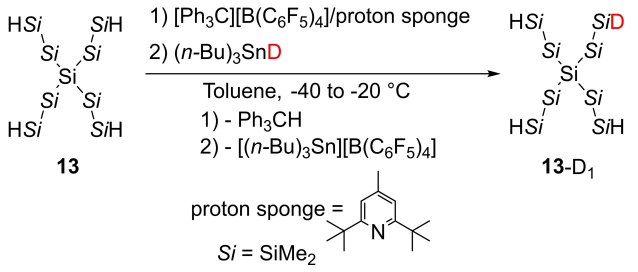

Scheme 5. Synthesis and trapping reaction of monocation **9**.

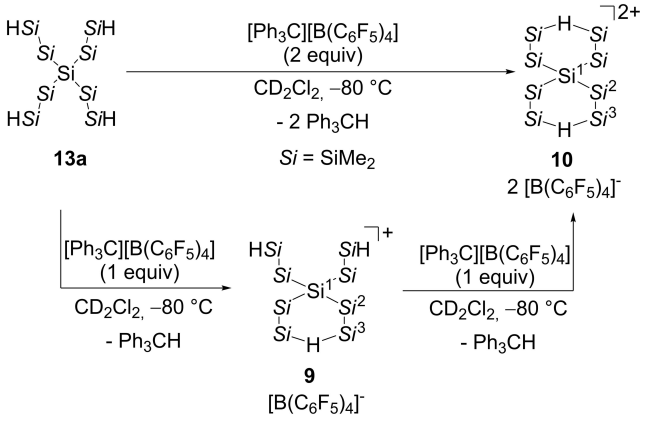

Scheme 6. Synthesis of **10**$[B(C_6F_5)_4]_2$ by hydride transfer reaction.

Similarly, the reaction of silyl borate **9**$[B(C_6F_5)_4]$ with one additional equivalent of trityl borate occurred immediately, even at T = −80 °C (Scheme 6). This suggests that the second hydride transfer from silyl cation **9** to trityl cation is fast, which contrast reports on the related carbosilane based dications **4**–**7**, which are formed only at elevated temperatures and extended reaction times.[14,30] The NMR spectroscopic investigations verify that both reactions give the same product, **10**$[B(C_6F_5)_4]_2$, which decomposes in dichloromethane at temperatures higher than T = −80 °C. The NMR spectroscopic data indicate the high symmetry of the obtained oligosilanylsilyl dication **10** (Table 1). Two sharp signals of equal intensity for only two magnetically different $SiMe_2$ groups are detected in the ^{1}H NMR spectrum at δ^1H = 0.55 and 0.89. Similar to cation **8**, the resonance (δ^1H = 0.81) of the bridging Si–H–Si hydrogen atom is observed by ^{1}H,^{29}Si HMQC NMR spectroscopy (Figure S90). The ^{13}C{^{1}H} NMR spectrum of the reaction product also shows only two signals (Figure S87). In the ^{29}Si{^{1}H} NMR spectrum, three singlet signals are detected at δ^{29}Si = −121.4 (Si^1), −34.4 (Si^2) and 88.1 (Si^3) (Figure 6). The latter splits in the hydrogen-coupled ^{29}Si NMR spectrum into a doublet with a coupling constant of $^1J_{Si,H}$ = 41 Hz (Figure 6, insert). The spectroscopic assignment is supported by ^{29}Si NMR chemical shift calculations for a DFT-optimized molecular structure of **10** (Table 1).

Comparison of the NMR spectroscopic parameters of the cations **8**–**10** reveals ^{29}Si NMR chemical shifts for the Si-H–Si silicon atoms in a very narrow range between $\delta^{29}Si^3$ = 87–89 (Table 1). The $^1J_{Si,H}$ coupling constants in these Si–H–Si bridges

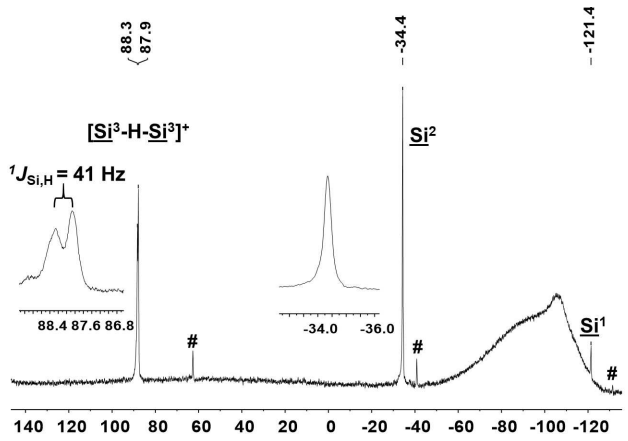

Figure 6. ^{29}Si NMR spectrum of **10**$[B(C_6F_5)_4]_2$ (CD_2Cl_2, 99.31 MHz, −80 °C, # = unidentified side-products).

are small ($^1J_{Si,H}$ = 31–41 Hz) as expected from the reduced bond order.[10,14] Finally, the ^{1}H NMR chemical resonances of the bridging hydrogen atoms in cations **8** ($\delta^{29}Si^1$ = 0.73 in CD_2Cl_2) and in dication **10** ($\delta^{29}Si^1$ = 0.81 in CD_2Cl_2) are found in a confined spectral region (Table 1). These NMR spectroscopic parameters are in the typically range reported for cationic 3c2e Si–H–Si bridges.[6] Interestingly, the presence of two positive charges in dication **10** does not influence its NMR parameters in any significant manner when compared to the monocationic silyl species **8** and **9**.

For all three cations, the good agreement between calculated and experimental ^{29}Si NMR chemical shifts is a sign of the quality of the molecular structures predicted by the DFT calculations. This allows a detailed discussion of structural and energetic parameters based on the DFT results. Cation **8** adopts a chair-like conformation of the Si_5H ring, with a bent symmetric Si–H–Si bond (α(Si–H–Sj) = 158°), both silicon atoms are separated by 319 pm and the Si–H bond length is 163 pm. These structural parameters are typical for silane-stabilized silylium ions[6] and similar values are obtained for the 3c2e Si–H–Si groups of cations **9** and **10** (see Supporting Information for details). The strength of the Si–H–Si bond in silyl cation **8** is predicted to be 81 kJ mol^{-1} as calculated from the energy difference between an artificial linear silylium ion **16** and Si–H–Si bridged cation **8** (Scheme 7, see Figure S121 for computed structures).

For cation **9**, we located several cyclic Si–H–Si bridged conformers of very similar energy. The maximal free enthalpy

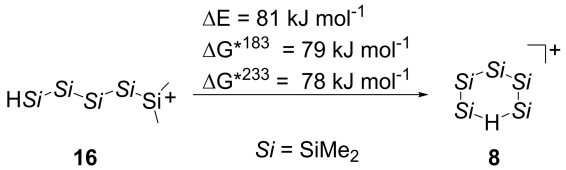

Scheme 7. Calculated energy gain by Si–H–Si bond formation of cation **8** (at M06-2X/6-311 + G(d,p)).

difference at T = −90 °C between these conformers is ΔG^{*183} = 17 kJ mol^{-1} (see Table S6) Compared to the isomeric silylium ion with an open structure (**17**), the conformer of **9a** of lowest energy is stabilized by ΔG^{*183} = 90 kJ mol^{-1} (Figure 7). In agreement with the NMR data, no interactions between the $[Si–H–Si]^+$ moiety and the two remaining Si–H functionalities are evident in the computed structure **9a**.

A transition state **TS1** for the intramolecular hydride transfer (Scheme 4) was located 27 kJ mol^{-1} above the conformer of lowest energy (Figure 7). **TS1** is characterized by a pentacoordinated silicon atom that adopts a trigonal-bipyramidal environment with the approaching and leaving Si–H groups in the apical positions (antarafacial arrangement, Figure 8). The computed activation barrier for this process agrees with the activation energy of 31 kJ mol^{-1} that was estimated based on the experimental VT ^{29}Si NMR data (Figure 3).

Additionally, an alternative transition state **TS2** for the intramolecular hydride transfer, which interchanges the Si–H groups in a suprafacial process was located (Figure 8). This transition state is markedly higher in energy ($\Delta G^{*+,183}$ = 61 kJ mol^{-1}) and was hence ruled out (Figure S124). The intramolecular antarafacial process involving **TS1** with its pentacoordinated silicon atom agrees well with the similar structural motif suggested by Nikonov and co-workers for the arene based silyl cation **2** (Figure 1).[25,26]

For dication **10**, the calculations predict the expected spirocyclic structure of C_2 point group symmetry (Figure 9).

The first Si–H–Si group stabilizes dication **18** by 85 kJ mol^{-1} compared to its non-bridged isomer **19**. Interestingly, dication **10** with two Si–H–Si bridges is lower in energy by additional 120 kJ mol^{-1} compared to dication **18** (Figure 10, Figure S121). This strong stabilization rules out the possibility for hydrogen exchange between the two Si–H–Si groups and is in qualitative agreement with the static structure of **10** detected by NMR spectroscopy in solution. A comparison with the isostructural carbodication **20** synthesized by Sorensen is interesting.[40] In contrast to the silicon species **10**, carbodication **20** undergoes a

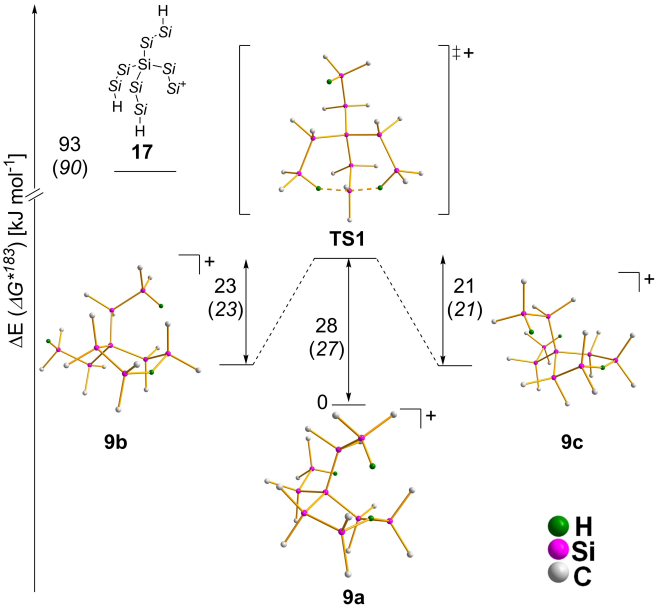

Figure 7. Part of the potential energy surface of **9** that shows the intramolecular hydride transfer in **9** (Scheme 4) (ΔE: electronic energy; ΔG^{*183}: Gibbs energy at 183K, both calculated at M06-2X/6-311 + G(d,p)).

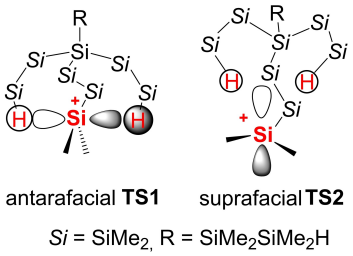

Figure 8. Schematic representation of the orbital interactions in the different transition states **TS1** and **TS2**.

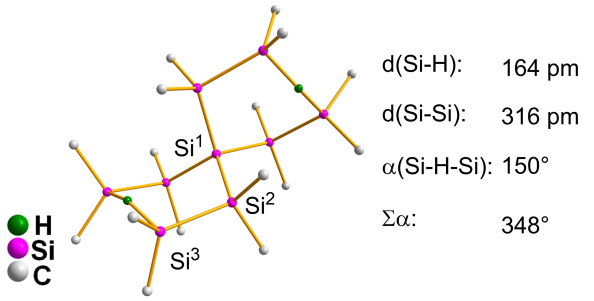

Figure 9. Computed C_2-symmetric structure of dication **10** and important parameters of the Si–H–Si bridge (at M06-2X/6-311 + G(d,p), all hydrogen atoms but the Si–H atoms are omitted for clarity, Σα : sum of the bond angles at Si^3 involving its three carbon substituents).

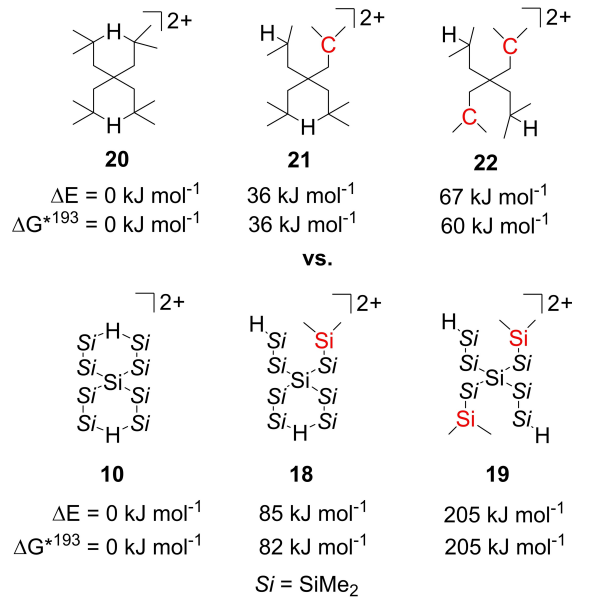

Figure 10. Comparison of the relative energies of carbodication **20** and silyl dication **10** with their non-bridged isomers. Tricoordinated carbon or silicon units are marked in red (ΔE: electronic energy; ΔG^{*193}: Gibbs energy at 193K, both calculated at M06-2X/6-311 + G(d,p))

rapid mutual exchange between the two C–H–C groups via a non-hydrogen bridged cations, in agreement with the much smaller calculated stabilization of **20** by the hydrogen bridges (29–36 kJ mol^{-1} per C–H–C bridge, Figure 10, Table S4, Figure S122).

Conclusion

The high utility of 3c2e Si–H–Si bridges to stabilize otherwise short-lived and highly reactive cationic oligosilane species at low temperatures was demonstrated. NMR data and the quantum mechanical derived structural parameters of cation **8** are very close to those determined for previously carbon based *bis*silylhydronium ions, such as **1** and **4**; however, the high reactivity and the thermal instability of the persila-analogue **8** is remarkable. The installation of additional hydridodimethylsilyl groups as in the branched cation **9** leads to a highly dynamic situation due to the fast interchange between Si–H groups coordinated to the silylium ion and free Si–H groups. This intramolecular Si–H group exchange proceeds via an associative mechanism with a very low barrier of approx. 30 kJ mol^{-1} along a pentacoordinated transition state. The intramolecular process studied for cation **9** serves as a general model also for intermolecular $[R_3Si–H–SiR_3]^+/R_3SiH$ group exchange in solutions of silylium ions in silanes.[19] It is interesting to note that beside this dynamic process, there is no interaction between the free Si–H groups and the cationic Si–H–Si bridge in the sense of polyagostic interaction in the ground state of cation **9**.

The second hydride transfer reaction between trityl cation and silyl cation **9** is remarkably facile. Even at −80 °C, it proceeds immediately to completion and yields exclusively dication **10**. This suggests that the second ionization step occurs at silane groups that are spatially separated from the positively charged $[Si–H–Si]^+$ moiety and that the existing and the evolving cation are also electronically isolated by the oligosilane backbone. This is also supported by the close agreement of the NMR spectroscopic parameter for the cationic $[Si–H–Si]^+$ units in monocations **8** and **9** compared to those of dication **10**. The formation of two independent $[Si–H–Si]^+$ groups confers to **10** a high conformational stability. The mutual exchange of the Si–H groups is excluded due to the high binding energy of 85–120 kJ mol^{-1} between the individual silylium ions and the silane unit. This distinguishes dication **10** from the corresponding dicarbocation **20**, which undergoes fast $C–H/C^+$ exchange due to the lability of the 3c2e $[C–H–C]^+$ bond.

The immediate synthesis of the silane-stabilized *bis*silylium ion **10** at low temperature contrasts recent results by the Oestreich group, who reported the preparation of carborate-stabilized *bis*silylium ions **5**–**7** by hydride transfer from carbon-tethered *bis*silanes at room temperature with reaction times up to several days.[30] In the case of compound **7**, it is not completely clear whether the rate-retarding factor is the stability of the Si–H–Si bridge of the intermediate *bis*silylhydronium carborate or its low solubility in the applied solvent. Our approach using tetrahydridosilanes as precursors and forming independently two silane-stabilized silylium ions is of advantage in respect of reaction temperature and time. *Bis*silylium ion **10** is a new example of a bidentate Lewis acid with largely unquenched silylium-ion character.[27–29] The two intramolecular $[Si–H–Si]^+$ units provide two electronically independent, highly Lewis acidic centers in one molecule. We expect this arrangement to be highly favorable for future catalytic application, for example, in hydrodefluorination reactions, and we will transfer it to other more robust molecular frameworks.[6,41,42]

Experimental Section

All hydride transfer reactions were performed as NMR experiments following the same protocol. The specified amount of $[Ph_3C][B(C_6F_5)_4]$ was directly weighted into an NMR tube which was then evacuated for 30 min and gently flushed with nitrogen. In the NMR tube, $[Ph_3C][B(C_6F_5)_4]$ was then dissolved in the respective NMR solvent and the resulting solution was cooled to the temperature needed for the NMR experiment using a cooling bath. Subsequently, the hydrogen-substituted silane, dissolved in the used NMR solvent, was slowly added by syringe. The addition proceeded slowly so that the silane-containing solution cooled down while it went down on the glass walls of the cooled NMR tube. In this way, biphasic mixtures were obtained. The NMR tube was sealed, removed from the cooling bath, and thoroughly mixed. The mixing proceeded as fast as possible so that a warming-up of the reaction mixture was minimized. Directly after mixing, the NMR tube was put back into the cooling bath, transferred into the precooled spectrometer and measured.

The handling of the NMR tubes was performed in specially designed glassware that allowed for the evacuation of the NMR tube and the subsequent handling under nitrogen. To guarantee a good thermal conduction between cooling bath and the solution in the NMR tube, the room between the glassware and the inlying NMR tube was filled with *n*-hexane.

Acknowledgements

The authors thank Prof. Dr. C. Marschner and Dr. J. Baumgartner (TU Graz) for many helpful discussions. All computations were performed at the HPC Cluster CARL, located at the University of Oldenburg (Germany) and funded by the DFG through its Major Research Instrumentation Program (INST 184/157-1 FUGG) and the Ministry of Science and Culture (MWK) of the Lower Saxony State. Open Access funding enabled and organized by Projekt DEAL.

Conflict of Interest

The authors declare no conflict of interest.

Data Availability Statement

The data that support the findings of this study are available in the supplementary material of this article.

Keywords: Lewis acids · NMR spectroscopy · oligosilanes · silicon · silyl cations

[1] L. Greb, *Chem. Eur. J.* **2018**, *24*, 17881–17896.
[2] J. B. Lambert, Y. Zhao, *Angew. Chem. Int. Ed. Engl.* **1997**, *36*, 400–401.
[3] T. Müller, Y. Zhao, J. B. Lambert, *Organometallics* **1998**, *17*, 278–280.
[4] K.-C. Kim, C. A. Reed, D. W. Elliott, L. J. Mueller, F. Tham, L. Lin, J. B. Lambert, *Science* **2002**, *297*, 825–827.
[5] A. Schäfer, M. Reißmann, S. Jung, A. Schäfer, W. Saak, E. Brendler, T. Müller, *Organometallics* **2013**, *32*, 4713–4722.
[6] H. F. T. Klare, L. Albers, L. Süsse, S. Keess, T. Müller, M. Oestreich, *Chem. Rev.* **2021**, *121*, 5889–5985.
[7] S. Künzler, S. Rathjen, A. Merk, M. Schmidtmann, T. Müller, *Chem. Eur. J.* **2019**, *25*, 15123–15130.
[8] J. Y. Corey, R. West, *J. Am. Chem. Soc.* **1963**, *85*, 2430–2433.
[9] J. Y. Corey, *J. Am. Chem. Soc.* **1975**, *97*, 3237–3238.
[10] T. Müller, *Angew. Chem. Int. Ed.* **2001**, *40*, 3033–3036; *Angew. Chem.* **2001**, *113*, 3123–3126.
[11] A. Sekiguchi, Y. Murakami, N. Fukuya, Y. Kabe, *Chem. Lett.* **2004**, *33*, 530–531.
[12] L. Albers, S. Rathjen, J. Baumgartner, C. Marschner, T. Müller, *J. Am. Chem. Soc.* **2016**, *138*, 6886–6892.
[13] L. Albers, J. Baumgartner, C. Marschner, T. Müller, *Chem. Eur. J.* **2016**, *22*, 7970–7977.
[14] R. Panisch, M. Bolte, T. Müller, *J. Am. Chem. Soc.* **2006**, *128*, 9676–9682.
[15] A. Schäfer, M. Reißmann, A. Schäfer, M. Schmidtmann, T. Müller, *Chem. Eur. J.* **2014**, *20*, 9381–9386.
[16] J. B. Lambert, S. Zhang, *J. Chem. Soc. Chem. Commun.* **1993**, 383–384.
[17] J. B. Lambert, S. Zhang, S. M. Ciro, *Organometallics* **1994**, *13*, 2430–2443.
[18] M. Nava, C. A. Reed, *Organometallics* **2011**, *30*, 4798–4800.
[19] S. J. Connelly, W. Kaminsky, D. M. Heinekey, *Organometallics* **2013**, *32*, 7478–7481.
[20] W. E. Piers, A. J. V. Marwitz, L. G. Mercier, *Inorg. Chem.* **2011**, *50*, 12252–12262.
[21] A. Y. Houghton, J. Hurmalainen, A. Mansikkamäki, W. E. Piers, H. M. Tuononen, *Nat. Chem.* **2014**, *6*, 983–988.
[22] M. Oestreich, J. Hermeke, J. Mohr, *Chem. Soc. Rev.* **2015**, *44*, 2202–2220.
[23] H. Fang, M. Oestreich, *Chem. Sci.* **2020**, *11*, 12604–12615.
[24] J. Chen, E. Y.-X. Chen, *Angew. Chem. Int. Ed.* **2015**, *54*, 6842–6846; *Angew. Chem.* **2015**, *127*, 6946–6950.
[25] A. Y. Khalimon, Z. H. Lin, R. Simionescu, S. F. Vyboishchikov, G. I. Nikonov, *Angew. Chem. Int. Ed.* **2007**, *46*, 4530–4533; *Angew. Chem.* **2007**, *119*, 4614–4617.
[26] S. Tussupbayev, G. I. Nikonov, S. F. Vyboishchikov, *J. Phys. Chem. A* **2009**, *113*, 1199–1209.
[27] M. Melaimi, F. P. Gabbaï, in *Advances in Organometallic Chemistry, Vol. 53* (Eds.: R. West, A. F. Hill, F. G. A. Stone), Academic Press, **2005**, p. 61–99.
[28] W. E. Piers, G. J. Irvine, V. C. Williams, *Eur. J. Inorg. Chem.* **2000**, *2000*, 2131–2142.
[29] L. Schweighauser, H. A. Wegner, *Chem. Eur. J.* **2016**, *22*, 14094–14103.
[30] Q. Wu, A. Roy, G. Wang, E. Irran, H. F. T. Klare, M. Oestreich, *Angew. Chem. Int. Ed.* **2020**, *59*, 10523–10526; *Angew. Chem.* **2020**, *132*, 10609–10613.
[31] X. Sun, T. Simler, R. Yadav, R. Köppe, P. W. Roesky, *J. Am. Chem. Soc.* **2019**, *141*, 14987–14990.
[32] Y. Chen, J. Li, Y. Zhao, L. Zhang, G. Tan, H. Zhu, H. W. Roesky, *J. Am. Chem. Soc.* **2021**, *143*, 2212–2216.
[33] I. Fleming, R. S. Roberts, S. C. Smith, *J. Chem. Soc. Perkin Trans. 1* **1998**, 1209–1214.
[34] W. Uhlig, *Chem. Ber.* **1996**, *129*, 733–739.
[35] J. Hlina, C. Mechtler, H. Wagner, J. Baumgartner, C. Marschner, *Organometallics* **2009**, *28*, 4065–4071.
[36] K. E. Ruehl, K. Matyjaszewski, *J. Organomet. Chem.* **1991**, *410*, 1–12.
[37] A. Wallner, H. Wagner, J. Baumgartner, C. Marschner, H. W. Rohm, M. Köckerling, C. Krempner, *Organometallics* **2008**, *27*, 5221–5229.
[38] H. A. Fogarty, D. L. Casher, R. Imhof, T. Schepers, D. W. Rooklin, J. Michl, *Pure Appl. Chem.* **2003**, *75*, 999–1020.
[39] H. Stueger, G. Fuerpass, T. Mitterfellner, J. Baumgartner, *Organometallics* **2010**, *29*, 618–623.
[40] F. Sun, T. Sorensen, *J. Am. Chem. Soc.* **1993**, *115*, 77–81.
[41] H. F. T. Klare, M. Oestreich, *Dalton Trans.* **2010**, *39*, 9176–9184.
[42] J. C. L. Walker, H. F. T. Klare, M. Oestreich, *Nat. Chem. Rev.* **2020**, *4*, 54–62.

Manuscript received: December 3, 2021
Accepted manuscript online: December 9, 2021
Version of record online: December 30, 2021